2018

Nitro-fatty acids are formed in response to virus infection and are potent inhibitors of STING palmitoylation and signaling

Cathrine A. Miner
Washington University School of Medicine in St. Louis
Wei Qian
Washington University School of Medicine in St. Louis
Jonathan J. Miner
Washington University School of Medicine in St. Louis

Nitro-fatty acids are formed in response to virus infection and are potent inhibitors of STING palmitoylation and signaling

Anne Louise Hansen[a], Gregory J. Buchan[b], Michael Rühl[c], Kojiro Mukai[d], Sonia R. Salvatore[b], Emari Ogawa[d], Sidsel D. Andersen[a], Marie B. Iversen[a], Anne L. Thielke[a], Camilla Gunderstofte[a], Mona Motwani[e], Charlotte T. Møller[a], Andreas S. Jakobsen[a], Katherine A. Fitzgerald[e], Jessica Roos[f], Rongtuan Lin[g], Thorsten J. Maier[a,f], Raphaela Goldbach-Mansky[h], Cathrine A. Miner[i], Wei Qian[i], Jonathan J. Miner[i,j,k], Rachel E. Rigby[l], Jan Rehwinkel[l], Martin R. Jakobsen[a], Hiroyuki Arai[d,m], Tomohiko Taguchi[d,n,o], Francisco J. Schopfer[b], David Olagnier[a], and Christian K. Holm[a,1]

[a]Department of Biomedicine, Aarhus University, 8000 Aarhus C, Denmark; [b]Department of Pharmacology and Chemical Biology, University of Pittsburgh, Pittsburgh, PA 15213; [c]Department of Pharmaceutical Chemistry, Goethe University, 60438 Frankfurt am Main, Germany; [d]Department of Health Chemistry, Graduate School of Pharmaceutical Sciences, University of Tokyo, 113-0033 Tokyo, Japan; [e]Division of Infectious Diseases and Immunology, University of Massachusetts Medical School, Worcester, MA 01655; [f]Department of Anesthesiology, Intensive Care Medicine and Pain Therapy, University Hospital Frankfurt, Goethe University, 60590 Frankfurt am Main, Germany; [g]Lady Davis Institute, Department of Medicine, McGill University, H3T 1E2 Montreal, QC, Canada; [h]Translational Autoinflammatory Disease Studies Unit, National Institute of Allergy and Infectious Diseases, NIH, Bethesda, MD 20850; [i]Department of Medicine, Washington University School of Medicine in St. Louis, St. Louis, MO 63110; [j]Department of Molecular Microbiology, Washington University School of Medicine in St. Louis, St. Louis, MO 63110; [k]Department of Pathology and Immunology, Washington University School of Medicine in St. Louis, St. Louis, MO 63110; [l]Medical Research Council (MRC) Human Immunology Unit, University of Oxford, MRC Weatherall Institute of Molecular Medicine, Radcliffe Department of Medicine, John Radcliffe Hospital, Headington, OX3 9DS Oxford, United Kingdom; [m]Japan Agency for Medical Research and Development (AMED)-Core Research for Evolutionary Medical Science and Technology (CREST), Japan Agency for Medical Research and Development, 100-0004 Tokyo, Japan; [n]Laboratory of Organelle Pathophysiology, Department of Integrative Life Sciences, Graduate School of Life Sciences, Tohoku University, Sendai, 980-8578 Miyagi, Japan; and [o]AMED-Precursory Research for Innovative Medical Care (PRIME), Japan Agency for Medical Research and Development, 100-0004 Tokyo, Japan

Edited by Daniel B. Stetson, University of Washington, Seattle, WA, and accepted by Editorial Board Member Ruslan Medzhitov July 3, 2018 (received for review April 11, 2018)

The adaptor molecule stimulator of IFN genes (STING) is central to production of type I IFNs in response to infection with DNA viruses and to presence of host DNA in the cytosol. Excessive release of type I IFNs through STING-dependent mechanisms has emerged as a central driver of several interferonopathies, including systemic lupus erythematosus (SLE), Aicardi–Goutières syndrome (AGS), and stimulator of IFN genes-associated vasculopathy with onset in infancy (SAVI). The involvement of STING in these diseases points to an unmet need for the development of agents that inhibit STING signaling. Here, we report that endogenously formed nitro-fatty acids can covalently modify STING by nitro-alkylation. These nitro-alkylations inhibit STING palmitoylation, STING signaling, and subsequently, the release of type I IFN in both human and murine cells. Furthermore, treatment with nitro-fatty acids was sufficient to inhibit production of type I IFN in fibroblasts derived from SAVI patients with a gain-of-function mutation in STING. In conclusion, we have identified nitro-fatty acids as endogenously formed inhibitors of STING signaling and propose for these lipids to be considered in the treatment of STING-dependent inflammatory diseases.

nitro-fatty acids | STING | palmitoylation | IFN | SAVI

The adaptor molecule stimulator of IFN genes (STING) is central to production of type I IFN in response to cytosolic DNA (1–3). Accumulating evidence now points to STING as a source of severe pathology in human disease. Most recently, gain-of-function mutations in the gene encoding STING (*TMEM173*) have been shown to drive a systemic and debilitating inflammatory condition known as stimulator of IFN genes-associated vasculopathy with onset in infancy (SAVI) (4). Other inflammatory diseases, such as Aicardi–Goutières syndrome, familial chilblain lupus, and retinal vasculopathy with cerebral leukodystrophy, also seem to depend on induction of type I IFN via STING activation (5–9). The involvement of STING in human disease highlights the unmet demand for treatments that target the ability of STING to induce release of proinflammatory cytokines, including type I IFNs.

STING is a transmembrane adaptor protein that signals downstream of the DNA sensor cGMP-AMP synthase (cGAS). On binding of dsDNA, cGAS catalyzes the formation of the cGMP-AMP (cGAMP), which binds to and activates STING (10–12). Binding of cGAMP to STING leads to recruitment and phosphorylation of the signaling molecule TANK-binding kinase 1 (TBK1) (13). Next, TBK1 mediates phosphorylation of the transcription factor IFN regulatory factor 3 (IRF3), which translocates to the nucleus as homodimers to initiate transcription of several cytokine genes, including type I IFNs (IFN-α/β) (13). Structurally, human STING is composed of a membrane-associated N-terminal region (amino acids 1–137), which includes four predicted transmembrane helices

Significance

Several chronic inflammatory conditions have recently been shown to depend on abnormally high activity of the signaling protein stimulator of IFN genes (STING). These conditions include examples from systemic lupus erythematosus, Aicardi–Goutières syndrome, and STING-associated vasculopathy with onset in infancy. The involvement of STING in these diseases points to an unmet demand to identify inhibitors of STING signaling, which could form the basis of anti-STING therapeutics. With this report, we identify distinct endogenously formed lipid species as potent inhibitors of STING signaling—and propose that these lipids could have pharmaceutical potential for treatment of STING-dependent inflammatory diseases.

Author contributions: A.L.H., T.J.M., T.T., F.J.S., D.O., and C.K.H. designed research; A.L.H., G.J.B., M.R., K.M., S.R.S., E.O., S.D.A., M.B.I., A.L.T., C.G., C.T.M., A.S.J., J. Roos, R.L., C.A.M., W.Q., J.J.M., T.T., F.J.S., D.O., and C.K.H. performed research; M.M., K.A.F., R.G.-M., R.E.R., J. Rehwinkel, M.R.J., H.A., T.T., and F.J.S. contributed new reagents/analytic tools; A.L.H., G.J.B., M.R., K.M., S.R.S., E.O., J. Roos, R.L., C.A.M., J.J.M., T.T., F.J.S., D.O., and C.K.H. analyzed data; and A.L.H., D.O., and C.K.H. wrote the paper.

Conflict of interest statement: F.J.S. declares financial interest in Complexa Inc.

This article is a PNAS Direct Submission. D.B.S. is a guest editor invited by the Editorial Board.

[1]To whom correspondence should be addressed. Email: holm@biomed.au.dk.

This article contains supporting information online at www.pnas.org/lookup/suppl/doi:10.1073/pnas.1806239115/-/DCSupplemental.

Published online July 30, 2018.

and a relatively large cytosolic C-terminal domain (amino acids 138–379). The structure of the cytosolic domain has been solved by X-ray crystallography and has been identified as the site of cGAMP binding and TBK1 and IRF3 phosphorylation (14–17). By contrast, it is largely unknown how the N-terminal region and its four predicted transmembrane regions contribute to STING function. However, a recent study has identified N-terminal cysteine residues at positions 88 and 91 as targets of palmitoylation in response to stimulation with cytosolic dsDNA. Palmitoylation at Cys88/91 was important for STING-dependent phosphorylation of TBK1 in the trans-Golgi network (TGN) and thus, central to STING-dependent induction of type I IFNs (18). It is currently unknown if palmitoylation at these cysteine residues can be targeted to inhibit STING signaling.

Recently, nitro-fatty acids (NO_2-FAs) have emerged as a group of bioactive lipids with antiinflammatory properties (19). At this stage, only a limited number of NO_2-FAs have been identified, and their importance in immune regulation during infection is poorly understood. Endogenous formation of NO_2-FAs is the result of nitrogen dioxide ($^{\bullet}NO_2$) addition preferentially to unsaturated fatty acids, such as conjugated linoleic acid (cLA) and oleic acid (OA), to form nitro-conjugated linoleic acid (NO_2-cLA) and nitro-oleic acid (NO_2-OA), respectively (20). During inflammation, formation of $^{\bullet}NO_2$ depends on the presence of inducible nitric oxide synthase (iNOS)-derived $^{\bullet}NO$, its autooxidation, or its reaction with oxygen species, including the NADPH oxidase (NOX)-derived superoxide anion $O_2^{\bullet-}$ (21). The $^{\bullet}NO_2$ reacts with lipid species to form NO_2-FAs (22) (Fig. 1*A*).

Formed NO_2-FAs have the ability to modify target proteins posttranslationally (*S*-nitro-alkylation) through Michael addition reactions. The thiol group on cysteine residues is a preferred target, and NO_2-FAs have been shown to modify the proteins, like Kelch-like ECH-associated protein 1, a repressor of the transcription factor Nuclear factor (erythroid-derived 2)-like 2 (Nrf2) (23), the signaling protein Peroxisome Proliferator-activated Receptor-γ (PPARγ) (24), and NF-κB (19). In these selected cases, nitro-alkylation leads to modulation of downstream signaling events, resulting in changes in metabolic, inflammatory, and antioxidative pathways.

Here, we show that NO_2-FAs can be formed in response to viral infection. Furthermore, we show that NO_2-FAs can inhibit STING signaling and the release of type I IFNs in response to stimulation with the STING agonists, dsDNA and cGAMP, in addition to infection with the DNA virus HSV-2. Mechanistically,

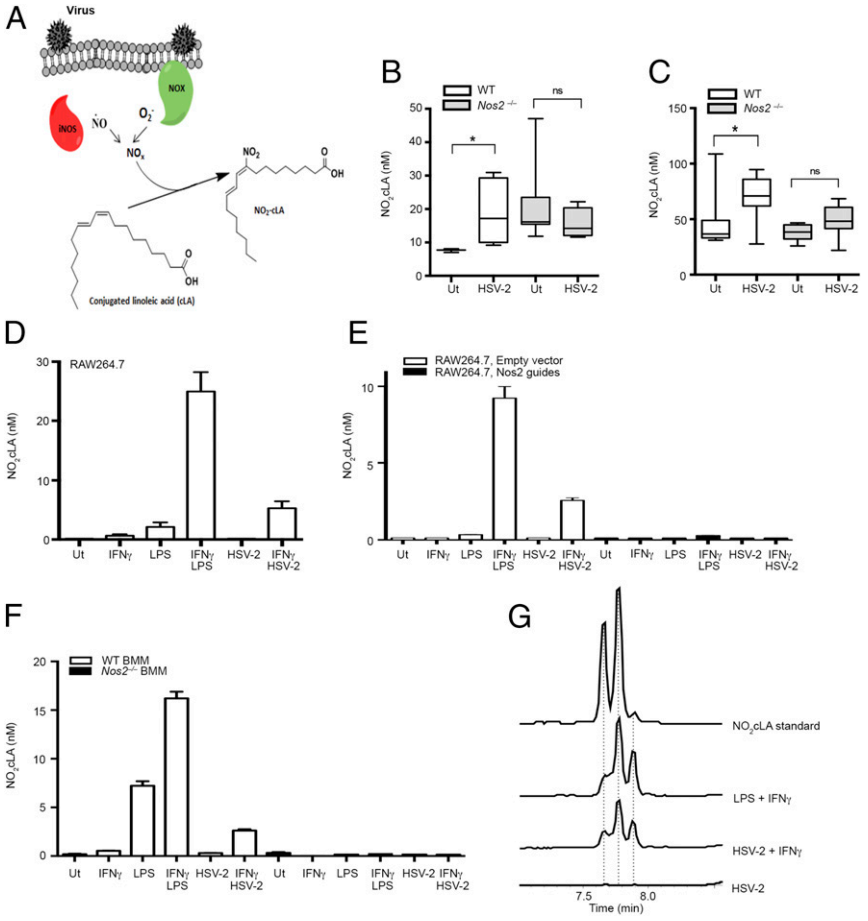

Fig. 1. NO_2-FAs are formed after HSV-2 infection. (*A*) Schematic of the formation of NO_2-FAs induced by iNOS/NOX production of NO species during virus infection. (*B*) Plasma and (*C*) vaginal lavages after inoculation with cLA (1 mM) in the vaginal lumen from WT and *Nos2*$^{-/-}$ C57BL/6 mice infected intravaginally with HSV-2 (6.7×10^4 pfu per mouse) were harvested at day 2 postinfection and analyzed for NO_2-cLA formation by mass spectrometry. One representative experiment of two independent experiments is shown. Data are represented as box/whiskers with (*B*) $n = 7$ mice per group and (*C*) $n = 8$ (untreated) or 12 (HSV-2 infected) mice per group. ns, Not significant. *$P < 0.05$ (unpaired Mann–Whitney *U* test). (*D*) RAW264.7 (WT) cells, (*E*) RAW264.7 control cells (empty vector) or RAW264.7 cells with CRISPR/Cas9-mediated deletion of *Nos2* expression, and (*F*) BMMs from WT or *Nos2*$^{-/-}$ mice were stimulated with combinations of IFN-γ (10 ng/mL), LPS (1 μg/mL), and HSV-2 (MOI 0.5) in the presence of cLA (100 μM). After 20 h of stimulation, supernatants were analyzed for NO_2-cLA formation by mass spectrometry. (*D*–*F*) Data represent three biological replicates in one experiment and are displayed as mean ± SEM. (*G*) Representative chromatogram showing coelution between samples (LPS + IFN-γ, HSV-2 + IFN-γ, and HSV-2) and standard, confirming the presence of NO_2-cLA.

NO_2-FAs directly modified STING through nitro-alkylation at the two adjacent cysteines at positions 88 and 91 (Cys88/91) and at an N-terminal histidine (His16), leading to a deregulation of STING palmitoylation and inhibition of STING signaling. Additionally, NO_2-FA treatment of immortalized fibroblasts from SAVI patients led to decreased STING-dependent type I IFN responses.

In conclusion, we show that endogenously formed NO_2-FAs are potent inhibitors of STING signaling and suggest that NO_2-FAs could be considered as a lipid-based treatment for STING-dependent inflammatory diseases.

Results

NO_2-FAs Are Formed in Response to Infection with Virus. As HSV infections are associated with release of high levels of reactive nitrogen species (25, 26), we tested if NO_2-FAs were formed in a model of vaginal HSV-2 infection, which induces a strong expression of iNOS (27). Expression of iNOS was most profoundly induced in leukocytes (CD45+ cells) at day 2 postinfection with HSV-2 (*SI Appendix*, Fig. S1); thus, plasma and vaginal lavages were collected at this time point. We found formation of the NO_2-FA species NO_2-cLA in response to HSV-2 infection in plasma (Fig. 1*B*) and in vaginal lavages after cLA inoculation (Fig. 1*C*). Despite biological variation between individual mice, the observed NO_2-cLA formation was significantly higher during HSV-2 infection in WT mice. Consequently, we report potent endogenous NO_2-FA formation after infection. Consistent with the concept of NO_2-FA generation being dependent on iNOS, a robust increase in NO_2-cLA formation was found in WT mice but not in mice deficient in the NO-forming enzyme iNOS ($nos2^{-/-}$) (Fig. 1 *B* and *C*). However, we did observe elevated basal levels of NO_2-cLA in plasma from $nos2^{-/-}$ mice, pointing to a compensatory but HSV-2–insensitive release of NO species by other enzymes (Fig. 1*B*). Formation of NO_2-cLA was also observed in vitro when infecting WT RAW264.7 cells with HSV-2 in the presence of the parent nonnitrated unsaturated lipid (cLA) serving as a template for NO_2-FA formation (Fig. 1*D*). Similarly, RAW264.7 cells (empty vector) (Fig. 1*E*) or bone marrow-derived macrophages (BMMs) from WT mice (Fig. 1*F*) likewise formed NO_2-cLA in response HSV-2 infection. In contrast, no NO_2-cLA formation was observed in iNOS-deficient RAW264.7 cells or BMMs (Fig. 1 *F* and *G*). Notably, the in vitro release of NO_2-cLA required the presence of IFN-γ (Fig. 1 *E* and *F*) beside iNOS-dependent $^{\bullet}NO$ formation (*SI Appendix*, Fig. S2). Remarkably, the combination of LPS and IFN-γ induced the highest in vitro release of both $^{\bullet}NO$-derived species (*SI Appendix*, Fig. S2) and NO_2-cLA formation (Fig. 1 *E*–*G*). Together, these results suggest that NO_2-cLA formation is occurring naturally in response to in vivo HSV-2 infection and after in vitro stimulation with LPS/IFN-γ and HSV-2/IFN-γ.

NO_2-FAs Inhibit Release of Type I IFN. Since NO_2-FAs have previously been reported to possess antiinflammatory properties (19), we next sought to test if various NO_2-FA species (NO_2-cLA, 9-NO_2-OA, and 10-NO_2-OA) could affect the release of type I IFNs to HSV-2 and HSV-2–derived stimuli as cytosolic dsDNA and cGAMP. We found that pretreatment with NO_2-FA led to highly reduced induction of type I IFNs in response to HSV-2 in both THP-1 cells (Fig. 2*A*) and BMMs (Fig. 2*C*). Comparable reduction was observed after NO_2-FA treatment before stimulation with dsDNA in THP-1 cells (Fig. 2*B*) and in BMMs (Fig. 2*D*). Treatment with NO_2-FA species after HSV-2 infection also led to reduced release for the IFN-induced cytokine CXCL10 (*SI Appendix*, Fig. S3). In addition, release of the proinflammatory cytokine IL-6 was likewise decreased on NO_2-FA treatment in various cell types (*SI Appendix*, Fig. S4). NO_2-FA treatment also reduced the release of other proinflammatory cytokines induced via Toll-like receptor-dependent and RIG-I–like receptor-dependent pathways (*SI Appendix*, Fig. S5). By contrast, type I IFN release was largely unaffected after treatment with the nonnitrated parent lipids linoleic acid (LA) and oleic acid (OA). The effect of NO_2-FAs on cytokine production was independent of Nrf2 activation (*SI Appendix*, Fig. S6) and PPARγ pathway (*SI Appendix*, Fig. S7), as the NO_2-FAs retained their inhibitory effect in various Nrf2-deficient cells and in the presence of two different PPARγ inhibitors, respectively. Induction of type I IFNs by infection with DNA viruses, such as HSV-2, and by stimulation with dsDNA is highly dependent on the cGAS-STING pathway (10, 11, 28). We, therefore, hypothesized that NO_2-FAs could possibly inhibit signaling through this pathway. By immunoblotting, we showed that treatment with NO_2-FA species led to reduced phosphorylation of STING, TBK1, and IRF3 as well as to reduced formation of STING and IRF3 dimers after stimulation with either cGAMP (Fig. 2 *E* and *F* and *SI Appendix*, Fig. S8) or dsDNA (Fig. 2 *E* and *G*). Collectively, these results suggest that NO_2-FAs are able to reduce type I IFN levels prominently by affecting the cGAS-STING signaling pathway.

NO_2-FAs Bind STING and Block STING Palmitoylation. Interestingly, we noticed a subtle but consistent mobility shift of STING monomers under nonreducing conditions (Fig. 2 *E*–*G*). This observation could implicate STING as an NO_2-FA target. To investigate this further, cells were treated with biotinylated forms of one NO_2-FA species, 10-NO_2-OA, and subsequently subjected to immunoprecipitation. Excitingly, biotinylated 10-NO_2-OA readily precipitated STING, indicating a possible direct modification of STING (Fig. 3 *A* and *B*).

Encouraged by these results, human STING-transfected HEK293T cells were treated with 10-NO_2-OA. The precipitated and eluted STING protein was analyzed for NO_2-OA modifications by mass spectrometry. By this method, three sites of STING nitro-alkylation were identified: two adjacent cysteine residues at positions 88 and 91 in addition to a histidine residue at position 16 (Fig. 3 *C* and *D*). Common for all three sites is their location in close proximity to the predicted transmembrane helices of STING. Other than NO_2-OA, we observed NO-OA and NH_2-OA as additional modifications at cysteine residues due to reduction and laser desorption ionization, and we found one of the peptides partially and fully reduced and the other partially and nonreduced. None of these modified peptides were observed in the untreated sample (Fig. 3*C*). This observation is supported by experiments conducted with synthetic peptides. As previously described, no such reductions occurred at histidine residues. Additionally, we investigated the previously described modification of 200 Da (29), which confirmed our findings (*SI Appendix*, Figs. S10 and S11).

In resting state, STING resides in the endoplasmic reticulum (ER) membrane, but binding to cGAMP initiates its translocation to Golgi membrane (30). Palmitoylation of STING at Cys88/91 recently has been shown to be essential for STING clustering in the TGN and for the downstream STING signaling (18). We, therefore, speculated if the underlying mechanism for NO_2-FA–mediated inhibition of STING signaling could occur by preventing STING palmitoylation. For detection of palmitoylation, STING-KO mouse embryonic fibroblasts (MEF) expressing STING-EGFP were cultured in the presence of radio-labeled palmitate (^{3}H-palmitate) before stimulation with the mouse STING agonist DMXAA. Using GFP-specific antibodies, we precipitated STING and subsequently determined palmitoylation by measuring ^{3}H-palmitate using an autoradiograph. As previously reported (18), treatment with DMXAA led to an increase in incorporation of ^{3}H into STING (18). In contrast, pretreatment with 10-NO_2-OA, but not with OA, considerably inhibited this process (Fig. 3*E*). These results suggest that NO_2-FA–modified STING was unable to be palmitoylated after DMXAA stimulation. Since the palmitoylation of Cys88 and Cys91 of STING is stimulation dependent and likely occurs in the Golgi (18), Cys88 and Cys91 may be in the reduced form when STING is in the ER. We propose that treatment of cells with NO_2-FA before stimulation modifies Cys88 and Cys91 of STING through nitro-alkylation in the ER, preventing the normal palmitoylation process that occurs on these Cys residues at the

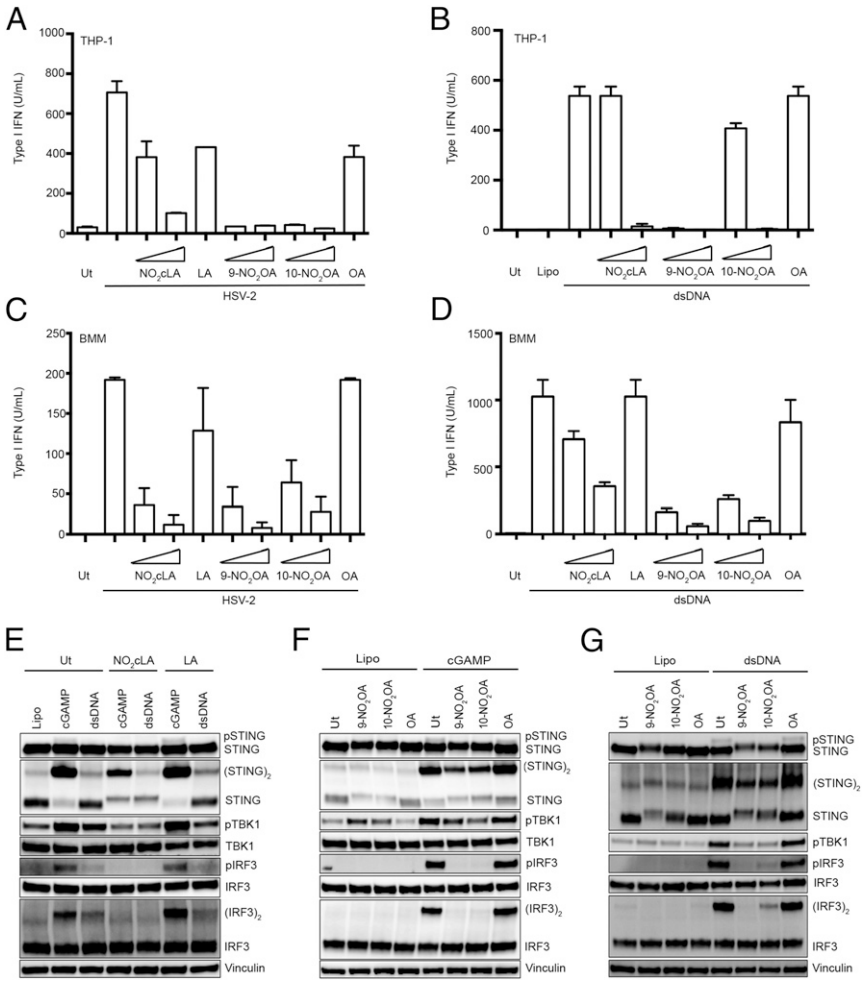

Fig. 2. NO_2-FAs suppress STING signaling and release of type I IFN. (*A* and *B*) THP-1 cells and (*C* and *D*) BMMs (WT mice) were treated with indicated NO_2-FAs (5–10 μM) or OA/LA (10 μM) 15 min before stimulation with dsDNA (4 μg/mL) or infection with HSV-2 (MOI 1) or left untreated (Ut). After 20 h, supernatants were harvested and analyzed for type I IFN. Data represent one of two independent experiments and are presented as mean ± SEM. (*E*–*G*) THP-1 cells were treated with NO_2-FAs (10 μM) or OA/LA (10 μM) 15 min before stimulation with cGAMP (4 μg/mL) or dsDNA (4 μg/mL) using Lipofectamine2000 (Lipo). After 3 h, lysates were separated by SDS/PAGE, and indicated proteins were detected by Western blotting using specific antibodies. STING and IRF3 dimers were detected using nondenaturing and nonreducing conditions. Vinculin was used as loading control.

Golgi. Palmitoylation of STING is important for STING clustering at the TGN and for phosphorylation of TBK1 at this location (18). For detailed investigation, we used STING-KO MEFs expressing STING-EGFP and stimulated with DMXAA. Costaining for pTBK1 and for TGN in the cells expressing STING-EGFP allowed us to test whether 10-NO_2-OA affected STING translocation to the TGN and/or phosphorylation of TBK1 by confocal microscopy. As expected, DMXAA stimulation induced translocation of STING to the perinuclear compartments, and STING colocalized with a TGN protein TGN38 (Fig. 3*F*, vehicle). pTBK1 signal showed up and partly colocalized with STING. On NO_2-FA treatment, in ∼30% of the cells, the perinuclear translocation of STING was unaffected, whereas this was markedly reduced in the remaining ∼70% of cells (Fig. 3*F*, 10-NO_2-OA). Strikingly, phosphorylation of TBK1 was inhibited regardless of whether STING translocated to the TGN. OA treatment, as a vehicle treatment, did not affect the perinuclear translocation of STING and the emergence of phosphorylated TBK1 (Fig. 3*F*, OA). In summary, NO_2-FAs directly modify and nitroalkylate STING at Cys88 and Cys91, resulting in inhibited palmitoylation and leading to the suppression of phosphorylation of TBK1.

NO_2-FAs Inhibit Release of Type I IFN in SAVI-Derived Fibroblasts. Gain-of-function mutations in the gene encoding STING (*TMEM173*) have been shown to drive pathology through excessive release of type I IFNs in SAVI (4). Since NO_2-FAs have been reported to be a well-tolerated treatment in humans (clinicaltrials.gov: NCT02460146 and NCT02313064), we wanted to determine if NO_2-FAs could decrease type I IFN responses in three SAVI patient-derived fibroblast cell lines, all bearing the N154S mutation. Indeed, we observed that release of type I IFN in response to stimulation with dsDNA was greatly inhibited in all three patients on treatment with NO_2-FA species (Fig. 4 *A*–*C*). In line, the expression of IFN-β as well as the expression of the two IFN-stimulated genes (ISGs), IFIT1 and ISG15, were likewise suppressed with NO_2-FA treatment (*SI Appendix*, Fig. S9). Furthermore, pTBK1, which was highly induced in the SAVI fibroblasts in response to cGAMP stimulation, was almost completely abolished by NO_2-FA treatment (Fig. 4*D*). As basal IFN-β production in fibroblasts was below the detection limit (Fig. 4 *A*–*C*), we used expression plasmids harboring gain-of-function STING mutants previously reported to cause SAVI (V174L, N154S, and V155M) to further test the treatment potential of NO_2-FAs. Indeed, NO_2-FA treatment could dampen the STING-dependent release of type IFN in a ligand-independent manner in this setup. In summary, these results imply the therapeutic potential of NO_2-FAs by dampening type I IFN levels in SAVI patient fibroblasts.

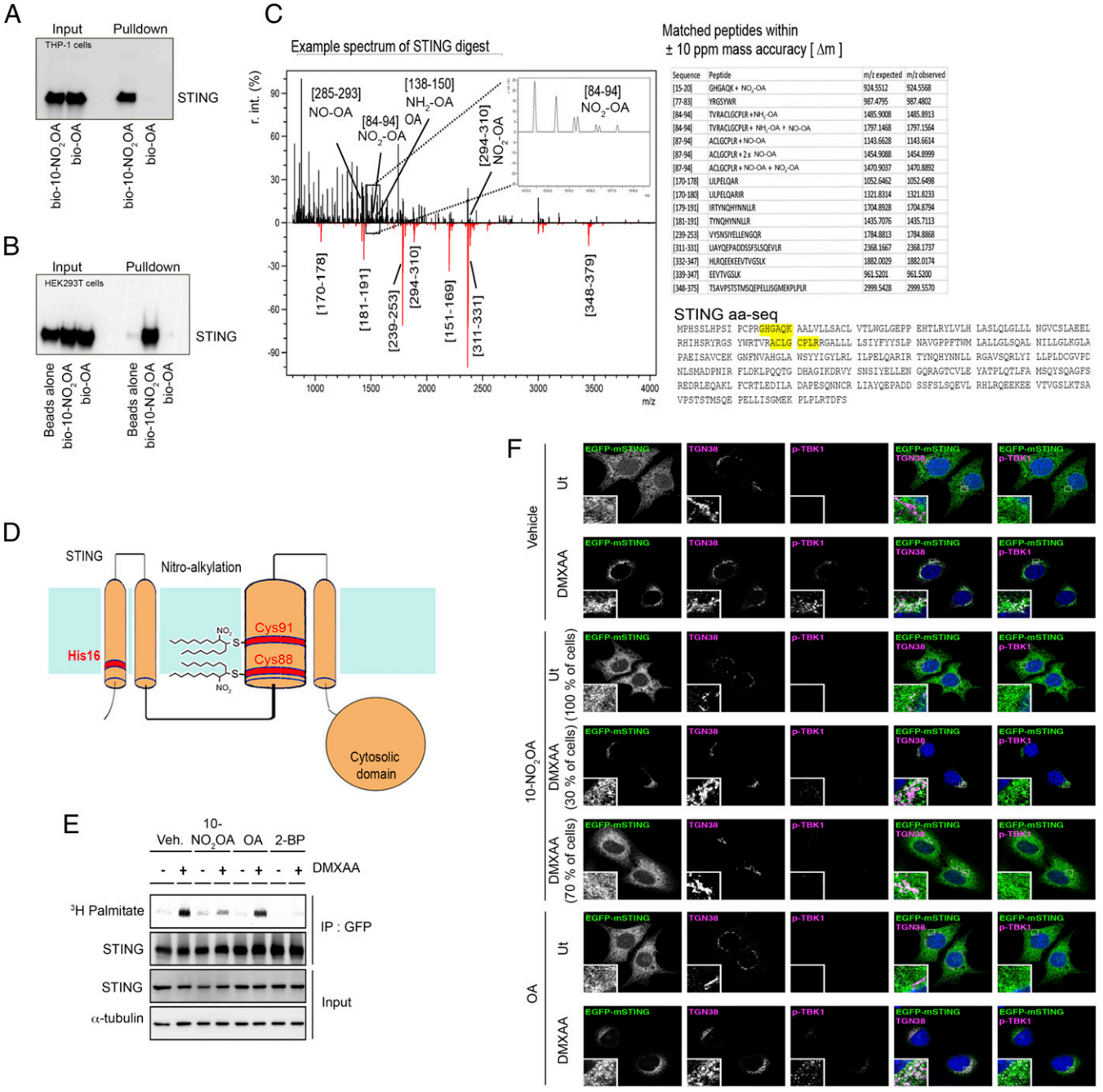

Fig. 3. NO_2-FAs directly modify STING to inhibit palmitoylation. (*A*) THP-1 cells with endogenous STING and (*B*) HEK293T cells transfected with expression plasmid for human STING plasmid (Flag tagged) were treated with biotinylated 10-NO_2-OA (10 μM) or biotinylated OA (10 μM). After 1.5-h incubation, lysates were precipitated using mixed magnetic Streptavidin beads. Eluates and input samples were separated by SDS/PAGE, and STING (α-Flag) was detected by Western blotting. Blots represent representative results from two independent experiments. (*C*) HEK293T cells transfected with an expression plasmid for human STING were treated with 10-NO_2-OA (10 μM). After 1.5 h, STING was precipitated using STING-specific antibody and analyzed for nitro-alkylation by mass spectrometry. Graphics display (*Left*) an example spectrum of STING digest: *Upper Left* in black shows NO_2-OA–treated STING, and *Lower Left* in red shows untreated STING as a comparison. r.int (%), relative intensity in %. (*Upper Right*) List of matched peptides. (*Lower Right*) STING amino acid sequence with peptides containing nitro-alkylation marked in yellow. Data are displayed from a single experiment. (*D*) Graphic illustration of the positions of nitro-alkylated STING residues. (*E*) Immortalized STING-KO MEFs expressing GFP-tagged STING were treated with 10-NO_2-OA (10 μM), OA (10 μM), 2-bromopalmitate, 2-BP (50 μM), or vehicle control for 1 h. Cells were washed and incubated with radio-labeled palmitate (^{3}H-palmitate) for 1 h before stimulation with DMXAA (25 mg/mL) or with vehicle control for an additional 1 h. Cells were lysed, and STING was precipitated (IP) using GFP-specific antibodies. Eluate and input were separated by SDS/PAGE and analyzed for contents of radio-labeled palmitate by autoradiography. STING was detected by immunoblotting, and α-tubulin was used as a loading control. Data displayed are from one of three independent experiments with same result. (*F*) Immortalized STING-KO MEFs expressing GFP-tagged STING were treated with 10-NO_2-OA (10 μM), OA (10 μM), or vehicle control as indicated before stimulation with DMXAA (25 mg/mL) or was left untreated (Ut) for 1 h. Cells that already express STING-GFP (green in merged panels) were fixed and stained for the TGN marker TGN38 (purple in merged panels) or pTBK1 (purple in merged panels), and the nuclei were stained with DAPI (blue in merged panels) and analyzed by confocal microscopy. The first three columns represent single stains of EGFP-STING, TGN38, and pTBK1, respectively. The last two columns represent merged pictures of EGFP-STING together with TGN38 and EGFP-STING together with pTBK1, respectively. *Insets* illustrate close-ups. Data represent two independent experiments.

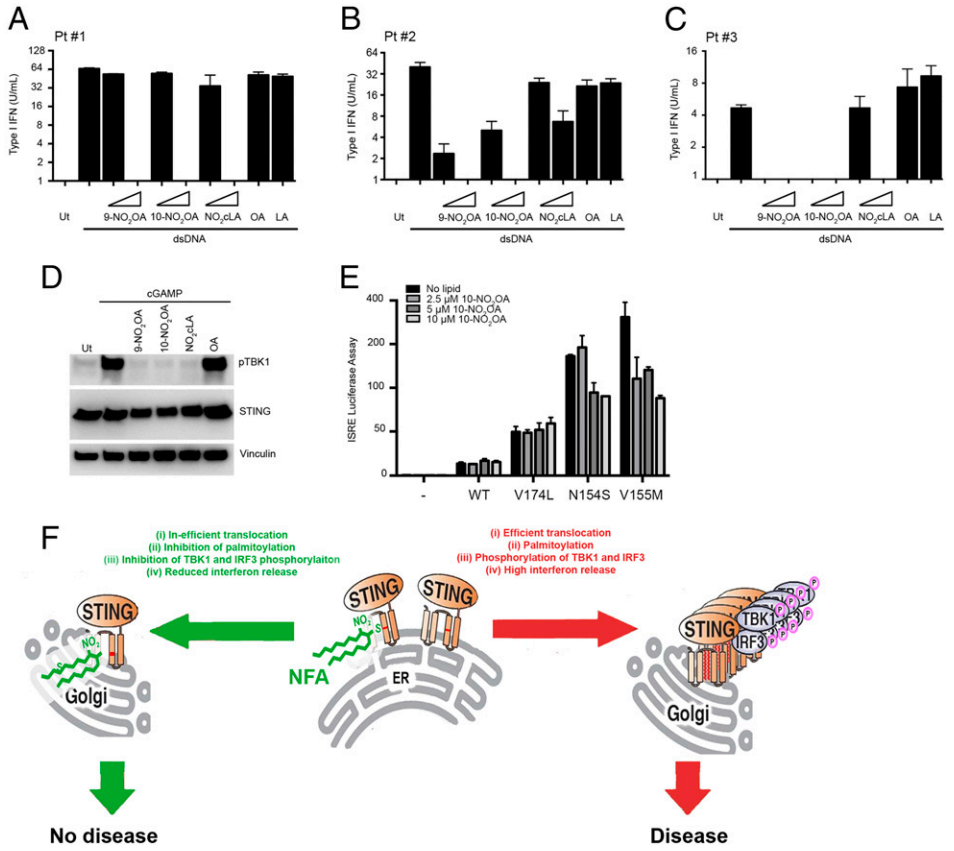

Fig. 4. NO_2-FAs inhibit release of type I IFN from SAVI fibroblasts. (*A–C*) Immortalized fibroblasts derived from three different SAVI patients were treated with indicated NO_2-FAs (5–10 μM) or OA/LA (10 μM) 15 min before stimulation with dsDNA (4 μg/mL). After 20 h, supernatants were harvested and analyzed for type I IFN. Data represent three biological replicates in one experiment of each donor and are displayed as mean ± SEM. (*D*) Immortalized fibroblasts from one SAVI patient (Pt #1) were treated with indicated NO_2-FAs (10 μM) or OA (10 μM) 15 min before stimulation with cGAMP (4 μg/mL). After 3 h, lysates were separated by SDS/PAGE, and indicated proteins were detected by Western blotting using specific antibodies. Vinculin was used as loading control. Data represent one experiment with one donor. (*E*) HEK293T cells were transfected with expression plasmids for WT STING, for three known gain-of-function STING mutations (V175L, N154S, V155M), or for no plasmid (–). Cells were treated with indicated 10-NO_2-OA (2.5–10 μM). Induction of IFN was assessed using the ISRE luciferase assay. Data are representative of two independent experiments and are displayed as means ± SEM. (*F*) Graphical abstract depicting how nitro-alkylation affects STING function. Modified from ref. 18.

Discussion

Gain-of-function mutations in STING can lead to a neonatal-onset systemic inflammatory condition characterized by severe cutaneous vasculopathy with extensive tissue loss and interstitial lung disease (SAVI) (4). Treatment options for SAVI patients or for patients with other STING-dependent inflammatory diseases are very limited. This is partly due to the absence of therapies that directly target STING signaling. This report identifies naturally occurring NO_2-FAs as potent inhibitors of STING signaling in human cells, including fibroblasts from SAVI patients. Thus, our data suggest that NO_2-FAs could be considered for trials aimed at treating patients with STING-dependent interferonopathies. This is further encouraged by the fact that NO_2-FAs are currently used in phase II trials for focal segmental glomerulosclerosis and pulmonary arterial hypertension and are here reported to be well-tolerated by the patients (clinicaltrials.gov: NCT02460146 and NCT02313064).

Our discovery that endogenous concentrations of NO_2-FAs are increased in response to virus-induced inflammation in mice together with the previous detection of NO_2-FA species and their adducts in human plasma and urine indicate that NO_2-FAs act as natural antiinflammatory mediators (31, 32). Testing this hypothesis is challenged by the difficulty to specifically eliminate NO_2-FAs from humans and even from mice. Antiinflammatory effects of the parent nonnitrated unsaturated lipids are widely reported (33). If part of these antiinflammatory effects is owing to the conversion into NO_2-FAs remains unknown. Notably, the parent nonnitrated unsaturated lipids have been documented to activate the PPARγ pathway (34)—also a known NO_2-FA target (24). The idea that highly inflammatory $^{\bullet}$NO-derived radicals, produced during inflammation, react with polyunsaturated lipids to form bioreactive antiinflammatory compounds is an attractive model for a built-in mechanism to counteract excessive inflammation. This hypothesis is supported by our demonstration that NO_2-FAs are formed in response to HSV-2 infection and in line with reported detection of NO_2-FAs formation in the peritoneum of mice after LPS injection (21, 35). Future research may focus on the importance of endogenous formation of NO_2-FAs to control inflammatory conditions in the context of either infection or noninfectious inflammatory disease.

Great advances have been made in understanding the structural basis for STING signaling in response to cytosolic dsDNA. Our data expand on this knowledge by identifying palmitoylation of STING (18) as a modification that can be targeted to inhibit STING signaling. This finding has considerable medical potential, as NO_2-FAs might either be used directly as antiinflammatory drugs or be used as a tool for designing highly efficient drugs that specifically target STING. In brief, our study opens up for embracing the functionality of the transmembrane helices of STING as targetable in future attempts to design antiinflammatory drugs.

In conclusion, we have discovered that endogenously formed NO_2-FAs can target STING signaling and reduce release of type I IFNs in both murine and human cells—including fibroblasts from patients with the STING-dependent interferonopathy SAVI. We, therefore, suggest that these lipids can be considered in the treatment of STING-dependent inflammatory diseases.

Materials and Methods

Animals. Animals received proper care in agreement with animal protocols approved by Animal Welfare Bodies at Health, Aarhus University, and we performed vaginal HSV-2 infection with ethical permission from the Animal Experiments Inspectorate, Danish Veterinary and Food Administration. Full details can be found in *SI Appendix, SI Materials and Methods*.

Cell Lines and Cell Culture. Full details can be found in *SI Appendix, SI Materials and Methods*.

Viruses and Reagents. Full details can be found in *SI Appendix, SI Materials and Methods*.

Vaginal HSV-2 Infection. Full details can be found in *SI Appendix, SI Material and Methods*.

Analytical Determination of NO_2-FAs Levels. Full details can be found in *SI Appendix, SI Materials and Methods*.

Cell Stimulation Setups. For in vitro HSV-2 stimulation, multiplicity of infection (MOI) at 0.5 or 1 was used.

For transfection setups, 4 μg/mL dsDNA (HSV-60; InvivoGen) and 4 μL/mL Lipofectamine2000 (Invitrogen) were used according to the manufacturer's instructions. Furthermore, cGAMP (Invitrogen) was used at a concentration of 4 μg/mL together 4 μL/mL Lipofectamine2000. Stimulation with cGAMP was performed using 4 μg/mL delivered to cells using Lipofectacmine2000 (Invitrogen).

Functional Type I IFN Assays. Murine IFN-α/β bioactivity was measured by an L929 cell-based bioassay as previously described (36). Human type I IFN bioactivity was quantified using the reporter cell line HEK-Blue IFN-α/β (InvivoGen) according to the manufacturer's instructions. SEAP levels were assessed by measuring OD at 620 nm on a microplate reader (ELx808; BioTEK).

Immunoprecipitation. Cells were lysed in Pierce RIPA lysing buffer (ThermoFisher Scientific) supplemented with 1× complete protease mixture inhibitor (Roche) and 5 IU mL^{-1} benzonase (Sigma). Lysate was collected and incubated with Pierce Streptavidin magnetic beads (ThermoFisher Scientific) for pulldown experiments of biotinylated NO_2-FA. Samples were washed once in PBS supplemented with 0.05% Tween-20, once with lysis buffer, and four times in 1 M KCl. Samples were eluted in 1× XT Sample Buffer (BioRad) and 1× XT reducing agent (BioRad) and further processed as described in *Immunoblotting*. Dynabeads Protein G (Invitrogen) was used for elution of STING for mass spectrometry analysis.

Detection of Nitro-Alkylation by Mass Spectrometry. Full details can be found in *SI Appendix, SI Materials and Methods*.

Metabolic Labeling with [^{3}H]-Palmitate. Full details can be found in *SI Appendix, SI Materials and Methods*.

Immunocytochemistry and Confocal Microscopy. They were previously described in ref. 18.

Luciferase Assay. For ARE-Luciferase assays, experiments were performed as previously described using the calcium phosphate transfection method. After 24 h of transfection and stimulation, luciferase activity was measured with a dual-luciferase reporter assay and a GloMax 20/20 luminometer as previously reported (37).

Immunoblotting. Full details can be found in *SI Appendix, SI Material and Methods*.

Primary Fibroblast Cell Lines Derived from SAVI Patients' Superficial Skin Biopsies. Patients with genetically confirmed SAVI were enrolled into the protocol (clinicaltrials.gov: NCT02974595) at the NIH between 2008 and 2015. The protocol was approved by the National Institute of Allergy and Infectious Diseases IRB at the NIH. Written informed consent was obtained from all participating patients or their legal guardians (R.G.-M.). Superficial research biopsies were obtained, and primary fibroblast cell lines were generated (4).

ACKNOWLEDGMENTS. We thank Søren R. Paludan for reagents used in this study. A.L.H. is supported by C. C. Klestrup and Wife Henriette Klestrup's Foundation, Director Jacob Madsen and Wife Olga Madsen's Foundation, The Bohemian Foundation, and Lily Benthine Lund's Foundation of 1.6.1978 in addition to a PhD fellowship from the Department of Health Sciences at Aarhus University. K.M. is supported by Japan Society for the Promotion of Science (JSPS) KAKENHI Grant JP17K15445 and ONO Medical Research Foundation. M.B.I. is supported by a Lundbeck postdoctoral fellowship. H.A. is supported by JSPS KAKENHI Grants JP17H06164 and JP17H06418, and AMED-CREST Grant 15652265. T.T. is supported by JSPS KAKENHI Grants JP16H04782 and JP15H05903 and AMED-PRIME. F.J.S. is supported by NIH Grants R01-GM125944 and R01-DK112854 and American Heart Association Grant 17GRN33660955. D.O. is supported by a Carlsbergfonden International Research Fellowship. C.K.H. is supported by The Hoerslev Foundation, Agnes and Poul Friis Foundation, The Brothers Hartmann's Foundation, Oda and Hans Svenningsen's Foundation, The Augustinus Foundation, and Hede Nielsen's Foundation.

1. Burdette DL, Vance RE (2013) STING and the innate immune response to nucleic acids in the cytosol. *Nat Immunol* 14:19–26.
2. Ishikawa H, Barber GN (2008) STING is an endoplasmic reticulum adaptor that facilitates innate immune signalling. *Nature* 455:674–678.
3. Ishikawa H, Ma Z, Barber GN (2009) STING regulates intracellular DNA-mediated, type I interferon-dependent innate immunity. *Nature* 461:788–792.
4. Liu Y, et al. (2014) Activated STING in a vascular and pulmonary syndrome. *N Engl J Med* 371:507–518.
5. Crow YJ, et al. (2006) Mutations in the gene encoding the 3′-5′ DNA exonuclease TREX1 cause Aicardi-Goutières syndrome at the AGS1 locus. *Nat Genet* 38:917–920.
6. Lee-Kirsch MA, et al. (2007) Mutations in the gene encoding the 3′-5′ DNA exonuclease TREX1 are associated with systemic lupus erythematosus. *Nat Genet* 39: 1065–1067.
7. Morita M, et al. (2004) Gene-targeted mice lacking the Trex1 (DNase III) 3′–>5′ DNA exonuclease develop inflammatory myocarditis. *Mol Cell Biol* 24:6719–6727.
8. Richards A, et al. (2007) C-terminal truncations in human 3′-5′ DNA exonuclease TREX1 cause autosomal dominant retinal vasculopathy with cerebral leukodystrophy. *Nat Genet* 39:1068–1070.
9. Stetson DB, Ko JS, Heidmann T, Medzhitov R (2008) Trex1 prevents cell-intrinsic initiation of autoimmunity. *Cell* 134:587–598.
10. Ablasser A, et al. (2013) cGAS produces a 2′-5′-linked cyclic dinucleotide second messenger that activates STING. *Nature* 498:380–384.
11. Diner EJ, et al. (2013) The innate immune DNA sensor cGAS produces a noncanonical cyclic dinucleotide that activates human STING. *Cell Rep* 3:1355–1361.
12. Li XD, et al. (2013) Pivotal roles of cGAS-cGAMP signaling in antiviral defense and immune adjuvant effects. *Science* 341:1390–1394.
13. Tanaka Y, Chen ZJ (2012) STING specifies IRF3 phosphorylation by TBK1 in the cytosolic DNA signaling pathway. *Sci Signal* 5:ra20.
14. Gao P, et al. (2013) Structure-function analysis of STING activation by c[G(2′,5′)pA(3′,5′)p] and targeting by antiviral DMXAA. *Cell* 154:748–762.
15. Huang YH, Liu XY, Du XX, Jiang ZF, Su XD (2012) The structural basis for the sensing and binding of cyclic di-GMP by STING. *Nat Struct Mol Biol* 19:728–730.
16. Yin Q, et al. (2012) Cyclic di-GMP sensing via the innate immune signaling protein STING. *Mol Cell* 46:735–745.
17. Zhang X, et al. (2013) Cyclic GMP-AMP containing mixed phosphodiester linkages is an endogenous high-affinity ligand for STING. *Mol Cell* 51:226–235.
18. Mukai K, et al. (2016) Activation of STING requires palmitoylation at the Golgi. *Nat Commun* 7:11932.
19. Cui T, et al. (2006) Nitrated fatty acids: Endogenous anti-inflammatory signaling mediators. *J Biol Chem* 281:35686–35698.
20. Bonacci G, et al. (2012) Conjugated linoleic acid is a preferential substrate for fatty acid nitration. *J Biol Chem* 287:44071–44082.
21. Vitturi DA, et al. (2015) Convergence of biological nitration and nitrosation via symmetrical nitrous anhydride. *Nat Chem Biol* 11:504–510.
22. Baker PR, Schopfer FJ, O'Donnell VB, Freeman BA (2009) Convergence of nitric oxide and lipid signaling: Anti-inflammatory nitro-fatty acids. *Free Radic Biol Med* 46: 989–1003.
23. Kansanen E, et al. (2011) Electrophilic nitro-fatty acids activate NRF2 by a KEAP1 cysteine 151-independent mechanism. *J Biol Chem* 286:14019–14027.
24. Li Y, et al. (2008) Molecular recognition of nitrated fatty acids by PPAR gamma. *Nat Struct Mol Biol* 15:865–867.
25. Fujii S, Akaike T, Maeda H (1999) Role of nitric oxide in pathogenesis of herpes simplex virus encephalitis in rats. *Virology* 256:203–212.
26. Wei XQ, et al. (1995) Altered immune responses in mice lacking inducible nitric oxide synthase. *Nature* 375:408–411.

27. Benencia F, et al. (2003) Nitric oxide and HSV vaginal infection in BALB/c mice. *Virology* 309:75–84.
28. Burdette DL, et al. (2011) STING is a direct innate immune sensor of cyclic di-GMP. *Nature* 478:515–518.
29. Gil M, et al. (2013) Inhibition of Mycobacterium tuberculosis PknG by non-catalytic rubredoxin domain specific modification: Reaction of an electrophilic nitro-fatty acid with the Fe-S center. *Free Radic Biol Med* 65:150–161.
30. Dobbs N, et al. (2015) STING activation by translocation from the ER is associated with infection and autoinflammatory disease. *Cell Host Microbe* 18:157–168.
31. Delmastro-Greenwood M, et al. (2015) Nitrite and nitrate-dependent generation of anti-inflammatory fatty acid nitroalkenes. *Free Radic Biol Med* 89:333–341.
32. Salvatore SR, et al. (2013) Characterization and quantification of endogenous fatty acid nitroalkene metabolites in human urine. *J Lipid Res* 54:1998–2009.
33. Reynolds CM, Roche HM (2010) Conjugated linoleic acid and inflammatory cell signalling. *Prostaglandins Leukot Essent Fatty Acids* 82:199–204.
34. Bassaganya-Riera J, Hontecillas R (2006) CLA and n-3 PUFA differentially modulate clinical activity and colonic PPAR-responsive gene expression in a pig model of experimental IBD. *Clin Nutr* 25:454–465.
35. Villacorta L, et al. (2018) In situ generation, metabolism and immunomodulatory signaling actions of nitro-conjugated linoleic acid in a murine model of inflammation. *Redox Biol* 15:522–531.
36. Iversen MB, et al. (2016) An innate antiviral pathway acting before interferons at epithelial surfaces. *Nat Immunol* 17:150–158.
37. Olagnier D, et al. (2017) Activation of Nrf2 signaling augments vesicular stomatitis virus oncolysis via autophagy-driven suppression of antiviral immunity. *Mol Ther* 25: 1900–1916.